Contribution of Diffusion to the Quenching by Oxygen of the Lowest Electronically Excited Singlet and Triplet States of Aromatic Molecules in Liquid Solution under High Pressure

Masami Okamoto,*,† Takahisa Tamai,‡ and Fujio Tanaka§

Faculty of Engineering and Design, Kyoto Institute of Technology, Matsugasaki, Sakyo-ku, Kyoto 606-8585, Japan, Laboratory of Physical Chemistry, Kyoto Institute of Technology, Matsugasaki, Sakyo-ku, Kyoto 606-8585, Japan, and College of Integrated Arts and Sciences, Osaka Prefecture University, Gakuen-cho, Sakai 599-8531, Japan

Received: April 30, 2002; In Final Form: November 4, 2002

The quenching by oxygen of the lowest electronically excited singlet (S_1) and triplet (T_1) states of five aromatic molecules in methylcyclohexane (MCH) at pressures up to 400 MPa was investigated. The apparent activation volume for the S_1 state, $\Delta V_q^{S\ddagger}$, at 0.1 MPa fell in the range from 14 to 16 cm^3/mol, which is significantly smaller than $\Delta V_\eta^{\ddagger}$ (25 cm^3/mol) determined from the pressure dependence of the solvent viscosity, η, whereas that for the T_1 state, $\Delta V_q^{T\ddagger}$, at 0.1 MPa changed from +6.1 (anthracene) to −15.2 cm^3/mol (triphenylene) and correlated approximately linearly with the triplet energy, E_T. However, $\Delta V_q^{T\ddagger}$ at 350 MPa was positive and almost independent of E_T (3−6 cm^3/mol). The pressure dependence of k_q^S was interpreted in the framework reported previously by us, and that of k_q^T was attributed to the contribution of diffusion to the quenching in which the encounter complex pair with singlet, triplet, and quintet spin multiplicities formed between the oxygen and T_1 state molecules is involved.

Introduction

It has been often believed that the lowest electronically excited singlet (S_1) and triplet (T_1) states of aromatic molecules are quenched by oxygen with nearly or fully diffusion-controlled rate.[1−4] The bimolecular quenching rate constant for the S_1 state, k_q^S, in a solvent with viscosity η, therefore, has been predicted approximately by the Debye equation for diffusion as follows:[1−5]

$$k_q^S = 8RT/\alpha\eta \qquad (1)$$

where α is 3000 and 2000 for the stick and slip boundary limits, respectively. For the quenching of the T_1 state by oxygen, it has been shown that the quenching rate constant, k_q^T, is nearly equal to $k_q^S/9$ because the encounter complex pairs with singlet,[1](MO$_2$)*, triplet, [3](MO$_2$)*, and quintet, [5](MO$_2$)*, multiplicities formed between the oxygen and T_1 state molecules, [3]M*, are involved in the quenching as shown in Scheme 1, [3,6] where k_{diff} is the rate constant for diffusion that is given approximately by eq 1. The branching ratio leading to the formation of singlet oxygen ($^1\Delta_g$) in the T_1 state, f_Δ^T, that is, the ratio of the rate constant for the formation of $^1\Delta_g$ ($=k_{diff}$ $k_{et}^T/(k_{-diff} + k_{et}^T)$) to k_q^T is unity for some anthracene derivatives ($f_\Delta^T = 1$),[7,8] whereas it is less than unity for some ketones[9,10] and close to unity for some aromatic compounds[11−16] in nonpolar solvents at 0.1 MPa. For the former case ($f_\Delta^T = 1$), the step of k_{ic}^T in Scheme 1 is closed, and $k_q^T = k_{diff}/9$ ($=k_q^S/9$) when $k_{et}^T \gg k_{-diff}$. For the latter case ($f_\Delta^T \neq 1$), $k_q^T = 4k_{diff}/9$ when $k_{et}^T \gg k_{-diff}$ and $k_{ic}^T \gg k_{-diff}$.

SCHEME 1

$$^3M^* + O_2(^3\Sigma_g^-) \underset{k_{-diff}}{\overset{(5/9)k_{diff}}{\rightleftarrows}} {}^5(MO_2)^*$$

$$^3M^* + O_2(^3\Sigma_g^-) \underset{k_{-diff}}{\overset{(3/9)k_{diff}}{\rightleftarrows}} {}^3(MO_2)^* \xrightarrow{k_{ic}^T} {}^1M + O_2(^3\Sigma_g^-)$$

$$^3M^* + O_2(^3\Sigma_g^-) \underset{k_{-diff}}{\overset{(1/9)k_{diff}}{\rightleftarrows}} {}^1(MO_2)^* \xrightarrow{k_{et}^T} {}^1M + O_2(^1\Delta_g)$$

Porter et al.[6] have studied the dependence of triplet energy, E_T, on k_q^T for various aromatic hydrocarbons, and found that k_q^T is maximal and constant for the molecules with $1.0 \times 10^4 < E_T < 1.5 \times 10^4$ cm^{-1} and decreases for those with $E_T > 1.6 \times 10^4$ cm^{-1}. They also found that the reaction probabilities (k_q^T/k_{diff}) increase in polar or viscous solvents by changing solvent at 0.1 MPa.

In general, because the application of high pressure can change significantly the solvent viscosity without changing temperature and solvent, the studies at high pressure have given us important information for the quenching with nearly or fully diffusion-controlled rate. Previously, we showed that the quenching rate constant by oxygen of the S_1 and T_1 states of some anthracene derivatives is close to a diffusion-controlled rate and found that k_q^T/k_q^S increases with increasing pressure.[17,18] Furthermore, for apparently nonfluorescent 9-acetylanthracene,[19] it was found that the branching ratio of the T_1 state in Scheme 1, f_Δ^T, is unity and independent of pressure up to 400 MPa in nonpolar solvents. It was also found that k_q^T/k_q^S, where k_q^S is the fluorescence quenching rate constant for 9,10-dimethylanthracene that is assumed to be equal to k_{diff}, increases over 1/9, and approaches 4/9 with increasing pressure. It was concluded that the intersystem crossing between the encounter complex pairs is involved in the oxygen quenching of the T_1 state of 9-acetylanthracene at high pressure.

* To whom correspondence should be addressed.
† Faculty of Engineering and Design, Kyoto Institute of Technology.
‡ Laboratory of Physical Chemistry, Kyoto Institute of Technology.
§ Osaka Prefecture University.

10.1021/jp021086g CCC: $25.00
Published on Web 02/07/2003

TABLE 1: Values of $\Delta V_q^{S\ddagger}$(cm³/mol), α_0, α_1, and $k^{S,bim,0}$ for the Oxygen Quenching of the S_1 State in MCH at 25 °C[a]

	k_q^S [b]/10^{10} M^{-1} s^{-1}	$\Delta V_q^{S\ddagger}$	α_0	α_1/P^{1-}	$k^{S,bim,0}/10^{10}$ M^{-1} s^{-1}
anthracene	2.87[c]	14.2 ± 0.9[c]			
pyrene	2.72[d]	15.6 ± 0.4[d]	530 ± 30	−360 ± 90	3.6 ± 0.7
			(440 ± 20)[c]		(2.4 ± 0.4)[d]
DBZA	2.20	14.6 ± 0.6	510 ± 30	−280 ± 120	2.5 ± 0.5
CHR	2.54	15.6 ± 0.6	510 ± 30	−370 ± 130	3.1 ± 0.7
TPH	2.42	14.7 ± 0.6	510 ± 50	−210 ± 170	2.9 ± 0.9

[a] The activation volume for solvent viscosity, $\Delta V_\eta^\ddagger$, determined by $(\partial \ln \eta/\partial P)_T = \Delta V_\eta^\ddagger/RT$ was 25 ± 1 cm³/mol at 0.1 MPa. [b] Values at 0.1 MPa. The errors were evaluated to be about 8% for DBZA, CHR, and TPH. [c] References 17 and 18. [d] Reference 20.

Very recently, the quenching of the S_1 state of pyrene,[20−22] 9,10-dimethylanthracene,[22−24] and benzo[*a*]pyrene[25] by oxygen as well as heavy atom quenchers at high pressure was examined, and it was shown that k_q^S can be separated into the bimolecular rate constant for diffusion, k_{diff}, and that for the quenching, $k^{S,bim}$, in the solvent cage from the analysis of the pressure-induced solvent viscosity dependence of k_q^S. The similar analysis was successfully applied for the triplet−triplet annihilation of 2-acetonaphthone[26] that is believed to be diffusion-controlled.

In this work, the rate constants, k_q^S and/or k_q^T, for acridine, 1,2,5,6-dibenzanthracene, chrysene, phenanthrene, and triphenylene whose E_T ranges from 1.58×10^4 to 2.32×10^4 cm^{-1} were measured in methylcyclohexane at pressures up to 400 MPa and 25 °C, and k_q^S was separated into k_{diff} and $k^{S,bim}$. By using k_{diff} thus evaluated from the quenching of the S_1 state, the pressure dependence of the ratio of k_q^T to k_{diff}, k_q^T/k_{diff} was determined. From the results, together with the dependence of the triplet energy, E_T, on k_q^T by varying pressure, that is, varying solvent viscosity, the quenching mechanism by oxygen of the T_1 state was discussed.

Experimental Section

Acridine and phenanthrene (PHEN) (zone refined; Tokyo Kasei Co.) and 1,2,5,6-dibenzanthracene (DBZA; guaranteed grade; Wako Pure Chemicals Co.) were used as received. Chrysene (CHR; Aldrich Chemical Co.) and triphenylene (TPH; guaranteed grade; Wako Pure Chemicals) were recrystallized from benzene and ethanol twice, respectively. Methylcyclohexane solvent (MCH; spectroscopic grade; Dojin Pure Chemicals Co.) was used without further purification.

Transient absorption measurements at high pressure were performed by using an 8-ns pulse from a nitrogen laser (337.1 nm) for excitation and a xenon analyzing flash lamp positioned at right angles to the direction of the excitation pulse. The analyzing light intensities were monitored by a Hamamatsu R928 photomultiplier through a Ritsu MC-25N monochromator and the signal was digitized by using a Hewlett-Packard 54510A digitizing oscilloscope. Fluorescence decay curve measurements at high pressure were performed by using a 0.3-ns pulse from a PRA LN103 nitrogen laser for excitation. The fluorescence intensities were measured by a Hamamatsu R1635-02 photomultiplier through a Ritsu MC-25NP monochromator, and the resulting signal was digitized by using a LeCroy 9362 digitizing oscilloscope. All data were analyzed by using a NEC 9801 microcomputer, which was interfaced to the digitizers. The details about the associated high-pressure techniques have been described elsewhere.[27,28]

The concentrations of the samples were adjusted to give absorbances of ca. 0.8 (1 cm cell) at 337.1 nm for the triplet lifetime measurements and ca. 0.1 at the maximum wavelength of absorption for each compound for the fluorescence lifetime measurements. The latter minimizes reabsorption effects. The sample solutions were deoxygenated by bubbling nitrogen gas under nitrogen atmosphere, and the value of the concentration of dissolved oxygen in the air-saturated solvent reported previously[17] was used (2.5 mM at 0.1 MPa). The increase in the concentration of oxygen by applying high pressure was corrected by using the compressibility of solvent.[29−31]

Temperature was controlled at 25 ± 0.1 °C. Pressure was measured by a calibrated manganin wire or a Minebea STD-5000K strain gauge.

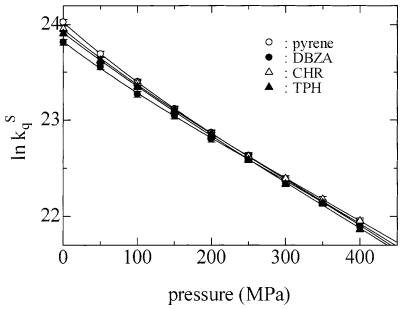

Figure 1. Pressure dependence of k_q^S for three aromatic molecules, together with that for pyrene,[20] in MCH and 25 °C. The pressure dependence of k_q^S for anthracene and some anthracene derivatives was reported elsewhere.[17,18] The solid lines were drawn by assuming that $\ln k_q^S = A + BP + CP^2$.

Results and Discussion

Pressure Dependence of the Quenching Rate Constant for the S_1 State, k_q^S. The decay curves of the S_1 state in the presence and absence of oxygen were analyzed satisfactorily by a single-exponential function. The lifetimes, τ_f^0, in the absence of oxygen were 46.9, 32.8, and 38.9 ns for CHR, DBZA, and TPH in MCH at 0.1 MPa, respectively; they are in a good agreement with those reported by other workers.[6] It was found that τ_f^0 is almost independent of pressure for the compounds examined. The quenching rate constant, k_q^S, for the S_1 state was determined by

$$1/\tau_f - 1/\tau_f^0 = k_q^S[O_2] \qquad (2)$$

where τ_f is the lifetime in air-saturated MCH ($[O_2] = 2.5$ mM at 0.1 MPa[17]). The values of k_q^S at 0.1 MPa are listed in Table 1. Figure 1 shows the pressure dependence of k_q^S for three aromatic molecules studied in this work, together with that for pyrene reported previously.[20] The apparent activation volume for k_q^S, $\Delta V_q^{i\ddagger}$ (i = S), determined by

$$(\partial \ln k_q^i/\partial P)_T = -\Delta V_q^{i\ddagger}/RT \; (i = S) \qquad (3)$$

is summarized in Table 1, together with that for solvent viscosity, η, $\Delta V_\eta^\ddagger$, determined from the pressure dependence of

SCHEME 2

$$^1M^* + O_2(^3\Sigma_g^-) \underset{k_{-diff}}{\overset{k_{diff}}{\rightleftharpoons}} {}^1(M^*O_2) \xrightarrow{k^S} {}^1M, {}^3M^*$$

η.[29−31] It is noted in Table 1 that $\Delta V_q^{S\ddagger}$ is almost independent of the fluorophores and significantly smaller than $\Delta V_\eta^\ddagger$. In our earlier works,[17,18,23] the large difference between $\Delta V_q^{S\ddagger}$ and $\Delta V_\eta^\ddagger$ for the nearly diffusion-controlled quenching was interpreted by the fractional power dependence of η on k_q^S as follows:

$$k_q^S = A\eta^{-\beta} \tag{4}$$

where A is independent of pressure, and $0 < \beta \leq 1$. The values of β determined from the plots of ln k_q^S and ln η for pyrene,[20] DBZA, CHR, and TP are 0.71 ± 0.01, 0.64 ± 0.02, 0.68 ± 0.02, and 0.69 ± 0.02, respectively; they are in good agreement with those for the oxygen quenching of the anthracene derivatives reported previously.[17,18,23] Recently, the observations that $\Delta V_q^{S\ddagger} < \Delta V_\eta^\ddagger$ was also found for the quenching of the S_1 state of pyrene, 9,10-dimethylanthracene, and benzo[*a*]pyrene by oxygen[20,22−25] and of pyrene, 9,10-dimethylanthracene, and benzo[*a*]pyrene by heavy atom quenchers,[21,23,25] and also for the excimer and exciplex formation,[32] and interpreted by the participation of diffusion to the quenching, that is, the observed quenching rate constant, k_q^S, involves the contribution of the bimolecular rate constant for diffusion, k_{diff}, and that for the quenching in the solvent cage, $k^{S,bim}$. Using this approach, k_{diff} is first evaluated, and then the oxygen quenching of the T_1 state is explored as described below.

Separation of k_q^S into k_{diff} and $k^{S,bim}$. The kinetic model of the quenching of the S_1 state by oxygen is expressed by[3,20,22−25] Scheme 2, where the step of k^S may occur in the solvent cage. On the basis of Scheme 2, the observed k_q^S is expressed by

$$k_q^S = \frac{k_{diff}k^S}{k_{-diff} + k^S} \tag{5}$$

In eq 5, $k_q^S = k_{diff}$ if $k^S \gg k_{-diff}$ and $k_q^S = k_{diff}\, k^S/k_{-diff}$ if $k_{-diff} \gg k^S$; the quenching occurs upon every encounter for the former case, whereas the quenching efficiency is less than unity for the latter case. When k_{diff} is assumed to be expressed by eq 1 (α in eq 1 is replaced by α^{ex}), we have[20,22−25]

$$\frac{1}{k_q^S} = \frac{1}{k^{S,bim}} + \frac{\alpha^{ex}}{8RT}\eta \tag{6}$$

where $k^{S,bim}$ is the bimolecular rate constant in the solvent cage at a given pressure, and defined by

$$k^{S,bim} = k^S\left(\frac{k_{diff}}{k_{-diff}}\right) \tag{7}$$

In eq 7, the pressure dependence of k_{diff}/k_{-diff} is given by that of the radial distribution function, $g(r_{M^*Q})$, at the closest approach distance (the encounter distance), r_{M^*Q} ($=r_{M^*} + r_Q$; the sum of the radius of $^1M^*$, r_{M^*}, and that of quencher, Q, r_Q), with hard spheres,[33] and hence, by introducing γ, the ratio of

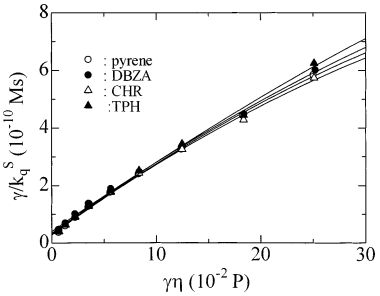

Figure 2. Plot of γ/k_q^S against $\gamma\eta$ for three aromatic molecules, together with that for pyrene,[20] in MCH at 25 °C. The solid lines were drawn by assuming that $\gamma/k_q^S = 1/k^{S,bim,0} + (1/8RT)\{\alpha_0(\gamma\eta) + \alpha_1(\gamma\eta)^2\}$ (see the text).

$g(r_{M^*Q})$ at P MPa to that at 0.1 MPa, $g(r_{M^*Q})/g(r_{M^*Q})_0$, eq 7 may be rewritten by

$$k^{S,bim} = \gamma k^S\left(\frac{k_{diff}}{k_{-diff}}\right)_0 = \gamma k^{S,bim,0} \tag{8}$$

where $k^{S,bim,0}$ is defined by $k^S(k_{diff}/k_{-diff})_0$ at 0.1 MPa. Thus, from eqs 6 and 8, we have

$$\frac{\gamma}{k_q^S} = \frac{1}{k^{S,bim,0}} + \frac{\alpha^{ex}}{8RT}\gamma\eta \tag{9}$$

According to eq 9, the plot of γ/k_q^S against $\gamma\eta$ should be linear. In fact, this approach has been successfully applied for some quenching systems.[20−22−25,32]

Recently, we showed that α^{ex} depends slightly on pressure and is expressed approximately by a polynomial in terms of $\gamma\eta$ for MCH with large pressure induced solvent viscosity dependence at a constant temperature.[24] In this work, α^{ex} was assumed by

$$\alpha^{ex} = \alpha_0 + \alpha_1(\gamma\eta) \tag{10}$$

Substituting eq 10 into eq 9, we have

$$\frac{\gamma}{k_q^S} = \frac{1}{k^{S,bim,0}} + \frac{1}{8RT}\{\alpha_0(\gamma\eta) + \alpha_1(\gamma\eta)^2\} \tag{11}$$

The plots of γ/k_q^S against $\gamma\eta$ are shown in Figure 2,[34] together that for pyrene reported previously.[20] All of the plots show good fittings with positive intercepts, indicating that the quenching competes with diffusion. The value of α^{ex} at a given pressure was determined from eq 10 by using the least squares coefficients, α_0, and α_1 in eq 11, and that of $k^{S,bim,0}$ from the least squares intercepts for the plots of γ/k_q^S against $\gamma\eta$ shown in Figure 2. The values of $k^{S,bim,0}$, and α_0 and α_1 are summarized in Table 1.

We can compare the observed k_q^S, k_q^S(obs), with k_q^S(cal) calculated by using $k^{S,bim}$ and k_{diff} according to eq 12 (see eqs 5 and 7) in which the values of $k^{S,bim}$ ($=\gamma k^{S,bim,0}$) and k_{diff} at a given pressure were evaluated from eqs 1 and 8, respectively, and examine the magnitude of the contribution of diffusion to the quenching

$$k_q^S(cal) = \frac{k^{S,bim}k_{diff}}{k^{S,bim} + k_{diff}} \tag{12}$$

Figure 3 shows the pressure dependence of k_{diff}, $k^{S,bim}$, k_q^S(obs), and k_q^S(cal). It is noted in Figure 3 that k_{diff} is close to $k^{S,bim}$ at

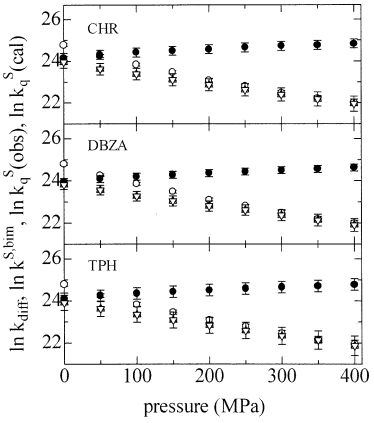

Figure 3. Pressure dependence of k_{diff}(○), $k^{S,bim}$(●), k_q^S(obs) (△), and k_q^S(cal) (▽) for three aromatic molecules in MCH at 25 °C.

TABLE 2: Values of k_q^T at 0.1 MPa, $\Delta V_q^{T\ddagger}$ (cm³/mol), for the Oxygen Quenching of the T_1 State in MCH and 25 °C, and the Triplet Energy, E_T

	$k_q^{T\,a}$ (10^9 $M^{-1}s^{-1}$)	$\Delta V_q^{T\neq}$ (0.1 MPa)	$\Delta V_q^{T\neq}$ (350 MPa)	$E_T{}^d$ (10^4 cm^{-1})
anthracene	3.76[b]	6.1 ± 0.1[b]	6 ± 1[b]	1.48
acridine	2.75	3.6 ± 0.3	6 ± 1	1.58
pyrene	2.49[c]	1.4 ± 0.5[c]	6 ± 1[c]	1.69
DBZA	1.57	−0.9 ± 0.4	4 ± 1	1.82
CHR	1.33	−3.6 ± 0.3	4 ± 1	2.00
PHEN	2.09	−4.7 ± 0.5	6 ± 1	2.17
TPH	0.60	−15.2 ± 0.6	3 ± 1	2.32

[a] Values at 0.1 MPa. The errors were evaluated to be about 3%. [b] References 17 and 18. [c] Reference 20. [d] References 1 and 6.

the lower pressure region, indicating that the quenching competes with diffusion. However, as pressure increases, that is, the solvent viscosity becomes higher, the difference between $k^{S,bim}$ and k_{diff} increases, hence, the quenching approaches a diffusion-controlled rate. Furthermore, the values of β for k_q^S(cal) in the fractional power dependence (eq 4) are 0.67 ± 0.04, 0.59 ± 0.04, 0.63 ± 0.04, and 0.64 ± 0.04 for pyrene, DBZA, CHR, and TP, respectively; they are in good agreement with those for k_q^S as mentioned above. As a result, it may be concluded that the quenching of the S_1 state examined in this work is nearly diffusion-controlled at the lower pressure region, being consistent with the conclusions for some other quenching systems in liquid solution as mentioned above.

Pressure Dependence of the Quenching Rate Constants for the T_1 State, k_q^T. The decay curves of the T_1 state in air-saturated MCH were analyzed satisfactorily by a single-exponential function for five aromatic molecules examined; the lifetimes, τ_T, at 0.1 MPa and 25 °C were 145.2, 254.8, 301.7, 191.6, and 665.0 ns for acridine, DBZA, CHR, PHEN, and TPH, respectively. The value of the quenching rate constant, k_q^T, of the T_1 state was determined by

$$1/\tau_T - 1/\tau_T^0 = k_q^T[O_2] \qquad (13)$$

where τ_T^0 is the lifetime of the T_1 state in the absence of oxygen. In the determination of k_q^T, $1/\tau_T^0$ in eq 13 is neglected because τ_T^0 is very long. The values of k_q^T at 0.1 MPa are listed in Table 2; they are in good agreement with the results reported previously.[6] The plots of ln k_q^T against pressure are shown in Figure 4, together with those for pyrene[20] and anthracene[17,18] reported previously. It is noted in Figure 4 that k_q^T at 0.1 MPa changes significantly from compound to compound, and its

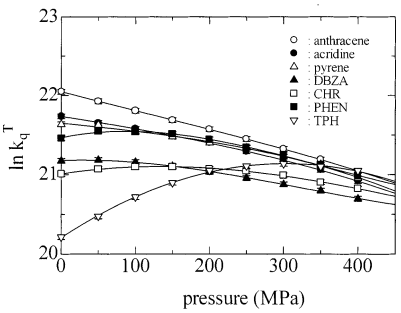

Figure 4. Pressure dependence of k_q^T for five aromatic molecules, together with that for pyrene[20] and anthracene,[17] in MCH at 25 °C. The solid lines were drawn by assuming that ln $k_q^T = A + BP + CP^2$.

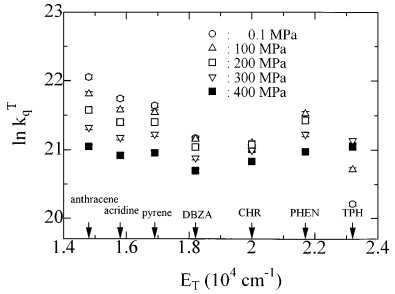

Figure 5. Triplet energy, E_T, dependence of k_q^T in MCH at five pressures.

pressure dependence is also influenced by the compounds examined; for the systems with higher k_q^T at 0.1 MPa, k_q^T decreases monotonically with increasing pressure, whereas for those with lower k_q^T at 0.1 MPa, the pressure dependence of k_q^T shows a maximum. The similar observations to the acridine/O_2 and DBZA/O_2 systems were found in the oxygen quenching of the T_1 state of anthracene,[17,18] 9-acetylanthracene,[19] and pyrene.[20] However, the pressure dependence of k_q^T with a maximum has not been observed to our knowledge. The activation volumes for k_q^T, $\Delta V_q^{T\ddagger}$, determined by eq 3 (i = T) are listed in Table 2. In Table 2, we can find that $\Delta V_q^{T\ddagger}$ changes from positive to negative, depending on the molecules examined. Such a trend shows a sharp contrast with that of $\Delta V_q^{S\ddagger}$ (see Table 1). It is also found that $\Delta V_q^{T\ddagger}$ decreases with decreasing k_q^T (0.1 MPa). These results for the T_1 state suggest the significant difference between the quenching of the S_1 and T_1 states.

Figure 5 shows the pressure dependence of the triplet energy, E_T, on k_q^T, where E_T value is listed in Table 2. The E_T dependence of k_q^T at 0.1 MPa is in a good agreement with that reported by Porter et al.,[6] who showed that k_q^T is maximal and constant for the molecules with $1.0 \times 10^4 < E_T < 1.5 \times 10^4$ cm^{-1} and decreases for those with $E_T > 1.6 \times 10^4$ cm^{-1}. However, the E_T dependence of k_q^T becomes smaller as pressure increases, and k_q^T is found to be almost independent of E_T at 400 MPa. The values of the activation volume, $\Delta V_q^{T\ddagger}$, at 350 MPa are listed in Table 2, together with those at 0.1 MPa. As seen in Table 2, $\Delta V_q^{T\ddagger}$ is positive and approximately independent of E_T at 350 MPa for all the compounds examined although it is strongly dependent on the T_1 state molecules at 0.1 MPa. From these facts, it is inferred that the pressure dependence of k_q^T is related to the solvent viscosity dependence of the rate processes associated with the oxygen quenching of the T_1 state.

Quenching Mechanism of the T_1 State by Oxygen. Because the oxygen quenching of the T_1 state may be nearly diffusion-controlled in nature, the ratio of k_q^T to the rate constant for diffusion, k_q^T/k_{diff} may be important. Figure 6 shows the plot of

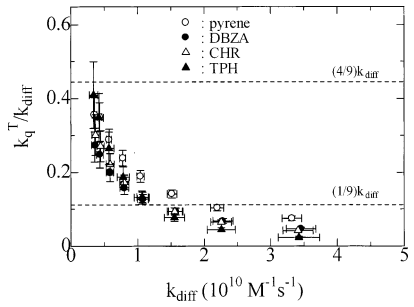

Figure 6. Plot of k_q^T/k_{diff} against k_{diff} for three aromatic molecules, together with that for pyrene,[20] in MCH.

k_q^T/k_{diff} against k_{diff}, where k_{diff} was determined from the values of α_0 and α_1, for three aromatic molecules (Table 1), together with that for pyrene.[20] According to Scheme 1, k_q^T/k_{diff} is given by

$$\frac{k_q^T}{k_{diff}} = \frac{1}{9}\frac{k_{et}^T}{k_{-diff} + k_{et}^T} + \frac{3}{9}\frac{k_{ic}^T}{k_{-diff} + k_{ic}^T} \qquad (14)$$

In eq 14, when the quenching is fully diffusion-controlled, we have two limiting cases; (i) for the case of $k_{et}^T \gg k_{-diff}$ and $k_{ic}^T \ll k_{-diff}$, $k_q^T/k_{diff} = 1/9$ and (ii) for the case of k_{et}^T, $k_{ic}^T \gg k_{-diff}$, $k_q^T/k_{diff} = 4/9$. When the quenching is reaction-controlled ($k_{-diff} \gg k_{et}^T$, k_{ic}^T), $k_q^T/k_{diff} = (k_{et}^T + 3k_{ic}^T)/9k_{-diff}$. As seen in Figure 6, k_q^T/k_{diff} is less than 1/9 at the lower pressure region, but approaches 4/9 over 1/9 as pressure increases for all the compounds examined. According to Scheme 1, the dependence of k_{diff} on k_q^T/k_{diff} shown in Figure 6 indicates that the quenching is reaction-controlled at the higher k_{diff} region and shifts to be fully diffusion-controlled (k_{et}^T, $k_{ic}^T \gg k_{-diff}$) as k_{diff} decreases. The branching ratio, f_Δ^T, at 0.1 MPa is reported to be close to unity for pyrene, CHR and DBZA in cyclohexane ($k_{ic} \sim 0$ in Scheme 1).[14] This evidence suggests that the maximum value of k_q^T/k_{diff} is 1/9 when f_Δ^T is independent of pressure.

We studied previously the pressure dependence of f_Δ^T (= 0.9 at 0.1 MPa in MCH) from the measurements of the yield of singlet oxygen, together with those of k_q^T and k_q^S for pyrene.[20] From the analysis of k_q^S by a similar method mentioned above, k_{diff} was evaluated at a given pressure. It was found that k_q^T/k_{diff} increases over 1/9 and approaches 4/9, whereas f_Δ^T decreases with increasing pressure. Thus, we concluded that the oxygen quenching of the T_1 state of pyrene is expressed by Scheme 1 ($k_{ic} \neq 0$) at pressures of about up to 250 MPa in MCH.[20] This was confirmed by the simulation of the plot of k_q^T/k_{diff} against k_{diff} on the basis of Scheme 1 ($k_{ic} \neq 0$).[20] However, above 250 MPa (in the higher solvent viscosity region), the root-mean-squares-errors (RMS) for the simulation is significantly large. As a result, it was inferred that the intersystem crossing between the encounter complex pairs is involved in the oxygen quenching of the T_1 state of pyrene,[20] although f_Δ^T at 0.1 MPa is close to unity.

Simulation for the Plot of k_q^T/k_{diff} against k_{diff}. As mentioned above, the branching ratio in the T_1 state, f_Δ^T, is known to be approximately unity for pyrene, CHR, and DBZA in cyclohexane at 0.1 MPa[14] although the error estimations were not made, suggesting that the maximum value of k_q^T/k_{diff} is 1/9 if f_Δ^T is independent of pressure. Generally, it is very difficult to measure f_Δ^T accurately at 0.1 MPa as well as at high pressure, especially, for the compounds with fluorescence because singlet oxygen is formed by the oxygen quenching of both the S_1 and T_1 states. In this section, we examined the simulation for the plot of k_q^T/k_{diff} against k_{diff} at the lower pressure region up to 200 MPa, based in Scheme 1 in order to obtain further insight into the quenching mechanism of the T_1 state.

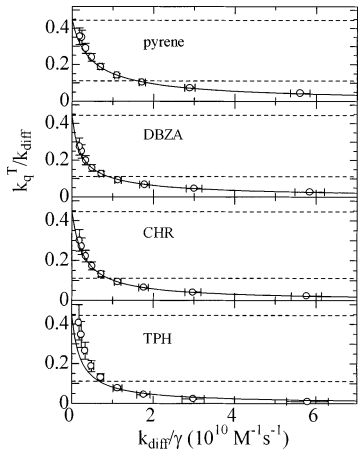

Figure 7. Plot of k_q^T/k_{diff} against k_{diff}/γ for three aromatic molecules, together with that for pyrene,[20] in MCH. The solid lines were drawn by the iterative nonlinear least-squares curve-fitting according to eq 15. The values of $k_{et}^{T,bim,0}$ and $k_{ic}^{T,bim,0}$ recovered are listed in Table 3 (see text).

TABLE 3: Values of $k_{et}^{T,bim,0}$, $k_{ic}^{T,bim,0}$, and f_Δ^T for the Oxygen Quenching of the T_1 State in MCH at 25 °C, Determined by the Simulation at Pressures up to 200 MPa

	$k_{et}^{T,bim,0}$ 10^{10} M^{-1} s^{-1}	$k_{ic}^{T,bim,0}$ 10^{10} M^{-1} s^{-1}	f_Δ^T (0.1 MPa)
pyrene	1.4 ± 0.3	0.35 ± 0.04	0.53 ± 0.21
	$(1.2 \pm 0.1)^a$	$(0.30 \pm 0.08)^a$	$(0.60 \pm 0.23)^a$
DBZA	1.1 ± 0.1	0.16 ± 0.01	0.66 ± 0.14
CHR	0.40 ± 0.3	0.27 ± 0.06	0.32 ± 0.30
TPH	0.39 ± 2.0	0.18 ± 0.36	0.41 ± 0.82

[a] Reference 20.

By the analogy with $k^{S,bim}$ (eq 8), the bimolecular rate constants for k_{et}^T and k_{ic}^T may be defined as follows: $k_{et}^{T,bim,0} = k_{et}^T(k_{diff}/k_{-diff})_0$ and $k_{ic}^{T,bim,0} = k_{ic}^T(k_{diff}/k_{-diff})_0$, and they are assumed reasonably to be independent of pressure. By using these relations, eq 14 may be rewritten by[20]

$$\frac{k_q^T}{k_{diff}} = \frac{1}{9}\frac{k_{et}^{T,bim,0}}{(k_{diff}/\gamma) + k_{et}^{T,bim,0}} + \frac{3}{9}\frac{k_{ic}^{T,bim,0}}{(k_{diff}/\gamma) + k_{ic}^{T,bim,0}} \qquad (15)$$

where f_Δ^T is given by the ratio of the first term to the full terms on the right-hand side. This approach by using the bimolecular rate constants such as $k_{et}^{T,bim,0}$ and $k_{ic}^{T,bim,0}$ was successfully applied for some quenching systems including the oxygen quenching of pyrene.[19,20,26] Figure 7 shows the plots of k_q^T/k_{diff} against k_{diff}/γ. The solid lines were drawn by the curve-fitting to eq 15 by using the data at pressures up to 200 MPa according to the iterative nonlinear least-squares method with two parameters. It is noted in Figure 7 that the fitting is well at the lower pressure region. The values of $k_{et}^{T,bim,0}$ and $k_{ic}^{T,bim,0}$ recovered are listed in Table 3, together with those of f_Δ^T at 0.1 MPa. As seen in Table 3, the values of $k_{et}^{T,bim,0}$ and $k_{ic}^{T,bim,0}$ for pyrene are in good agreement with those reported previously, in which k_{diff} was determined by assuming that α^{ex} is independent of $\gamma\eta$ (see eqs 9 and 10), and also the value of f_Δ^T at 0.1 MPa is fairly close to that determined experimentally ($f_\Delta^T = 0.9 \pm 0.3$) reported by us.[20]

In Table 3, $k_{et}^{T,bim,0}$ increases with decreasing E_T, being in agreement with the tendency of k_q^T, whereas $k_{ic}^{T,bim,0}$ is approximately independent of E_T. It is also found in Table 3 that $k_{et}^{T,bim,0}$ approaches $k_{ic}^{T,bim,0}$ for the T_1 state molecules with higher E_T. In eq 15, as pressure increases, k_{diff}/γ decreases significantly, and hence the contribution of the second term, which leads to the formation of O_2 ($^3\Sigma_g^-$), compared to the first one (O_2 ($^1\Delta_g$)) on the right-hand side of eq 15, increases; the values of f_Δ^T at 200 MPa were calculated to be 0.52 ± 0.08, 0.40 ± 0.08, 0.30 ± 0.20, and 0.36 ± 0.58 for pyrene, DBZA, CHR, and TPH, respectively. Thus, f_Δ^T decreases with increasing pressure because the contribution of the formation of O_2 ($^3\Sigma_g^-$) increases. Unfortunately, except for pyrene, there are no data of the pressure dependence of f_Δ^T for the T_1 state molecules that would allow further discussion at the present stage.

Finally, in the fitting of the plot of k_q^T/k_{diff} against k_{diff}/γ for TPH, the errors were found to be significantly large as noted in Figure 7 and Table 3. It should be also noticed that in the fittings on the basis of Scheme 1 by using the data at pressures up to 400 MPa, the root-mean-squares-errors (RMS) are significantly large. These facts suggest that Scheme 1 is not a suitable mechanism for the oxygen quenching of T_1 state at the higher pressure region. It seems likely that the intersystem crossing between the encounter complex pairs occurs at all of the pressure region examined although the magnitude of the contribution to k_q^T/k_{diff} and f_Δ^T depends on that of k_{et} and k_{ic} (Scheme 1) as well as the rate constant of the intersystem crossing between the encounter complex pairs. In fact, the fitting with using the quenching mechanisms involving the intersystem crossing leads to very low RMS for all of the T_1 state molecules examined at pressures up to 400 MPa.

Summary

The effect of pressure of the oxygen quenching of the S_1 and T_1 states of five aromatic molecules in methylcyclohexane was investigated. It was found that the rate constant, k_q^S, for the oxygen quenching of the S_1 state decreased monotonically for all of the compounds examined in this work. The apparent activation volume, $\Delta V_q^{S\ddagger}$, at 0.1 MPa for k_q^S fell in the range from 14 to 16 cm^3/mol, being independent of the compounds examined (Table 1). These results were satisfactorily interpreted in the framework reported previously by us[20,22−24] that the quenching is not fully but nearly diffusion-controlled, and k_q^S was separated into the bimolecular rate constant for diffusion, k_{diff}, and that for the quenching in the solvent cage, k_{bim} according to eq 11. The rate constant, k_q^T, for the oxygen quenching of the T_1 state at 0.1 MPa decreased with increasing the triplet energy E_T (Table 2), being in a good agreement with the results reported by Porter et al.[6] The pressure dependence of k_q^T showed a monotonical decrease and a maximum, depending on the compounds examined. The apparent activation volume, $\Delta V_q^{T\ddagger}$, at 0.1 MPa for k_q^T changed from +6.1 (anthracene) to −15.2 cm^3/mol (TPH) (Table 2), which were approximately linearly related to E_T. However, $\Delta V_q^{T\ddagger}$ at 350 MPa was positive and almost independent of E_T (3−6 cm^3/mol) (Table 2). By the simulation on the basis of Scheme 1 (eq 15), it was found that the formation (k_{diff}) and dissociation (k_{-diff}) of the encounter complex pairs are significantly retarded by the increase of solvent viscosity with pressure, whereas γ ($=(k_{diff}/k_{diff})/(k_{diff}/k_{diff})_0$) that is given by the ratio of the radial distribution function at contact at P MPa to that at 0.1 MPa increases moderately with pressure. It was also found that the magnitude of $k_{et}^{T,bim,0}$ and $k_{ic}^{T,bim,0}$ depends on E_T (Tables 2 and 3). As a result, the large variation of $\Delta V_q^{T\ddagger}$ at 0.1 MPa among the compounds examined is given by not only the pressure dependence of k_{diff}, but also that of the right-hand side of eq 15.

References and Notes

(1) Birks, J. B. *Photophysics of Aromatic Molecules*; Wiley-Interscience: New York, 1970; p 518.
(2) Birks, J. B. *Organic Molecular Photophysics*; Wiley: New York, 1973; p 403.
(3) Saltiel, J.; Atwater, B. W. *Advances in Photochemistry*; Wiley-Interscience: New York, 1987; Vol. 14, p 1.
(4) Ware, W. R. *J. Phys. Chem.* **1962**, *66*, 455.
(5) Rice, S. A. In *Comrehensive Chemical Kinetics. Diffusion-Limited Reactions*; Bamford, C. H., Tripper, C. F. H., Compton, R. G., Eds.; Elsevier: Amsterdam, 1985; Vol. 25.
(6) Gijzeman, O. L. J.; Kaufman, F.; Porter, G. *J. Chem. Soc., Faraday Trans.* 2 **1973**, *69*, 708.
(7) Wilkinson, F.; McGravey, D. J.; Olea, A. F. *J. Am. Chem. Soc.* **1993**, *115*, 12151.
(8) Olea, A. F.; Wilkinson, F. *J. Phys. Chem.* **1995**, *99*, 4518.
(9) Redmond, R. W.; Braslavsky, S. E. *Chem. Phys. Lett.* **1988**, *148*, 523.
(10) Darmanyan, A. P.; Foote, C. S. *J. Phys. Chem.* **1993**, *97*, 5032.
(11) McGravey, D. J.; Szekeres, P. G.; Wilkinson, F. *Chem. Phys. Lett.* **1992**, *199*, 314.
(12) Wilkinson, F.; McGravey, D. J.; Olea, A. F. *J. Phys. Chem.* **1994**, *98*, 3762.
(13) Wilkinson, F.; Abdel-Shafi, A. A. *J. Phys. Chem. A* **1997**, *101*, 5509.
(14) Usui, Y.; Shimizu, N.; Mori, S. *Bull. Chem. Soc. Jpn.* **1992**, *65*, 897.
(15) McLean, A. J.; McGarvery, D. J.; George Truscott, T.; Lambert, C. R.; Land, E. J. *J. Chem. Soc., Faraday Trans.* **1990**, *86*, 3075.
(16) Abdel-Shafi, A. A.; Wilkinson, F. *J. Phys. Chem. A* **2000**, *104*, 5747.
(17) Yasuda, H.; Scully, A. D.; Hirayama, S.; Okamoto, M.; Tanaka, F. *J. Am. Chem. Soc.* **1990**, *112*, 6847.
(18) Hirayama, S.; Yasuda, H.; Scully, A. D.; Okamoto, M. *J. Phys. Chem.* **1994**, *98*, 4609.
(19) Okamoto, M.; Tanaka, F.; Hirayama, S. *J. Phys. Chem.* **1998**, *102*, 10703.
(20) Okamoto, M.; Tanaka, F. *J. Phys. Chem. A* **2002**, *106*, 3982.
(21) Okamoto, M. *J. Phys. Chem. A* **2000**, *104*, 7518.
(22) Okamoto, M. *Int. J. Thermophys.* **2002**, *23*, 421.
(23) Okamoto, M.; Wada, O.; Tanaka, F.; Hirayama, S. *J. Phys. Chem. A* **2001**, *105*, 566.
(24) Okamoto, M. *Phys. Chem. Chem. Phys.* **2001**, *3*, 3696.
(25) Okamoto, M.; Wada, O. *J. Photochem. Photobiol. A* **2001**, *138*, 87.
(26) Okamoto, M.; Teratsuji, T.; Tazuke, Y.; Hirayama, S. *J. Phys. Chem. A* **2001**, *105*, 4574.
(27) Okamoto, M.; Teranishi, H. *J. Phys. Chem.* **1984**, *88*, 5644.
(28) Okamoto, M.; Teranishi, H. *J. Am. Chem. Soc.* **1986**, *108*, 6378.
(29) Bridgman, P. W. *Proc. Am. Acad. Arts. Sci.* **1926**, *61*, 57.
(30) Brazier, D. W.; Freeman, G. R. *Can. J. Chem.* **1969**, *47*, 893.
(31) Jonas, J.; Hasha, D.; Huang, S. G. *J. Chem. Phys.* **1979**, *71*, 15.
(32) Okamoto, M. *J. Phys. Chem. A* **2000**, *104*, 5029.
(33) Yoshimura, Y.; Nakahara, M. *J. Chem. Phys.* **1984**, *81*, 4080.
(34) The radial distribution function at the closest approach distance, $r_{M^*Q}(=r_{M^*}+r_Q)$ with the hard sphere assumption, $g(r_{M^*Q})$, is given by[33]

$$g(r_{M^*Q}) = \frac{1}{1-y} + \frac{3y}{(1-y)^2}\left(\frac{r_{red}}{r_S}\right) + \frac{2y^2}{(1-y)^3}\left(\frac{r_{red}}{r_S}\right)^2 \quad \text{(A-1)}$$

where $r_{red} = r_{M^*}r_Q/r_{M^*Q}$, and y is the packing fraction, given in terms of the molar volume of solvent, V_S, by

$$y = \frac{4N_A\pi r_S^3}{3V_S} \quad \text{(A-2)}$$

By using the values of r_S, r_{M^*}, and r_Q,[35] together with the data of the solvent density,[29−31] $g(r_{M^*Q})$ was calculated by eq A-1. In the plot of γ/k_q^S against $\gamma\eta$, the available data[29−31] of the solvent viscosity, η, was used.
(35) Bondi, A. *J. Phys. Chem.* **1964**, *68*, 441.